Combined polarized Raman and atomic force microscopy: *In situ* study of point defects and mechanical properties in individual ZnO nanobelts

Marcel Lucas,[1] Zhong Lin Wang,[2] and Elisa Riedo[1,a)]
[1]*School of Physics, Georgia Institute of Technology, Atlanta, Georgia 30332-0430, USA*
[2]*School of Materials Science and Engineering, Georgia Institute of Technology, Atlanta, Georgia 30332-0245, USA*

(Received 8 June 2009; accepted 23 June 2009; published online xx xx xxxx)

We present a method, polarized Raman (PR) spectroscopy combined with atomic Force microscopy (AFM), to characterize *in situ* and nondestructively the structure and the physical properties of individual nanostructures. PR-AFM applied to individual ZnO nanobelts reveals the interplay between growth direction, point defects, morphology, and mechanical properties of these nanostructures. In particular, we find that the presence of point defects can decrease the elastic modulus of the nanobelts by one order of magnitude. More generally, PR-AFM can be extended to different types of nanostructures, which can be in as-fabricated devices. © *2009 American Institute of Physics*. [DOI: 10.1063/1.3177065]

Nanostructured materials, such as nanotubes, nanobelts (NBs), and thin films, have potential applications as electronic components, catalysts, sensors, biomarkers, and energy harvesters.[1–5] The growth direction of single-crystal nanostructures affects their mechanical,[6–8] optoelectronic,[9] transport,[4] catalytic,[5] and tribological properties.[10] Recently, ZnO nanostructures have attracted a considerable interest for their unique piezoelectric, optoelectronic, and field emission properties.[1,2,11,12] Numerous experimental and theoretical studies have been undertaken to understand the properties of ZnO nanowires and NBs,[11,12] but several questions remain open. For example, it is often assumed that oxygen vacancies are present in bulk ZnO, and that their presence reduces the mechanical performance of ZnO materials.[13] However, no direct observation has supported the idea that point defects affect the mechanical properties of individual nanostructures.

Only a few combinations of experimental techniques enable the investigation of the mechanical properties, morphology, crystallographic structure/orientation and presence of defects in the same individual nanostructure, and they are rarely implemented due to technical challenges. Transmission electron microscopy (TEM) can determine the crystallographic structure and morphology of nanomaterials that are thin enough for electrons to transmit through,[4,14–17] but suffers from some limitations. For example, characterization of point defects is rather challenging.[14–17] Also, the *in situ* TEM characterization of the mechanical and electronic properties of nanostructures is very challenging or impossible.[15–17] Alternatively, atomic force microscopy (AFM) is well suited for probing the morphology, mechanical, magnetic, and electronic properties of nanostructures from the micron scale down to the atomic scale.[3,6,7,10] In parallel, Raman spectroscopy is effective in the characterization of the structure, mechanical deformation, and thermal properties of nanostructures,[18,19] as well as the identification of impurities.[20] Furthermore, polarized Raman (PR) spectroscopy was recently used to characterize the crystal structure and growth direction of individual single-crystal nanowires.[21]

Here, an AFM is combined to a Raman microscope through an inverted optical microscope. The morphology and the mechanical properties of individual ZnO NBs are determined by AFM, while polarized Raman spectroscopy is used to characterize *in situ* and nondestructively the growth direction and randomly distributed defects in the same individual NBs. We find that the presence of point defects can decrease the elastic modulus of the NBs by almost one order of magnitude.

The ZnO NBs were prepared by physical vapor deposition (PVD) without catalysts[14] and deposited on a glass cover slip. For the PR studies, the cover slip was glued to the bottom of a Petri dish, in which a hole was drilled to allow the laser beam to go through it. The round Petri dish was then placed on a sample plate below the AFM scanner, where it can be rotated by an angle φ, or clamped (see Fig. 1). The morphology and mechanical properties of the ZnO NBs were characterized with an Agilent PicoPlus AFM. The AFM was placed on top of an Olympus IX71 inverted optical microscope using a quickslide stage (Agilent). A silicon AFM probe (PointProbe NCHR from Nanoworld), with a normal cantilever spring constant of 26 N/m and a radius of about 60 nm, was used to collect the AFM topography and modulated nanoindentation data. The elastic modulus of the NBs was measured using the modulated nanoindentation method[22] by applying normal displacement oscillations at the frequency of 994.8 Hz, at the amplitude of 1.2 Å, and by varying the normal load. PR spectra were recorded in the backscattering geometry using a laser spot small enough (diameter of $1-2$ μm) to probe one single NB at a time. The incident polarization direction can be rotated continuously with a half-wave plate and the scattered light is analyzed along one of two perpendicular directions by a polarizer at the entrance of the spectrometer (Fig. 1). Series of PR spectra from the bulk ZnO crystals and the individual ZnO NBs were collected with varying sample orientation φ (the NBs are parallel to the incident polarization at $\varphi=0$), in the co- (parallel incident and scattered analyzed polarizations) and cross-polarized (perpendicular incident and scattered analyzed polarizations) configurations. For the ZnO NBs, additional series of PR spectra were collected where the incident

a)Electronic mail: elisa.riedo@physics.gatech.edu.

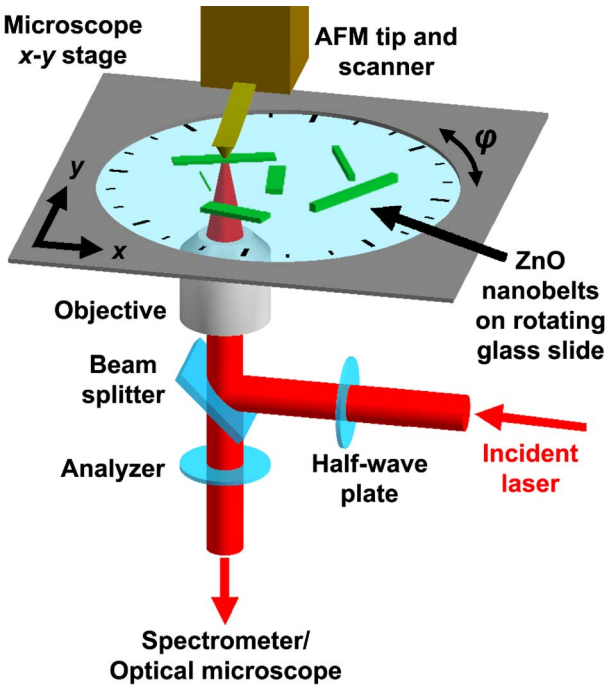

FIG. 1. (Color online) Schematic of the experimental setup, showing the path of the laser beam. The ZnO NBs are deposited on a glass slide, which is placed inside a rotating Petri dish.

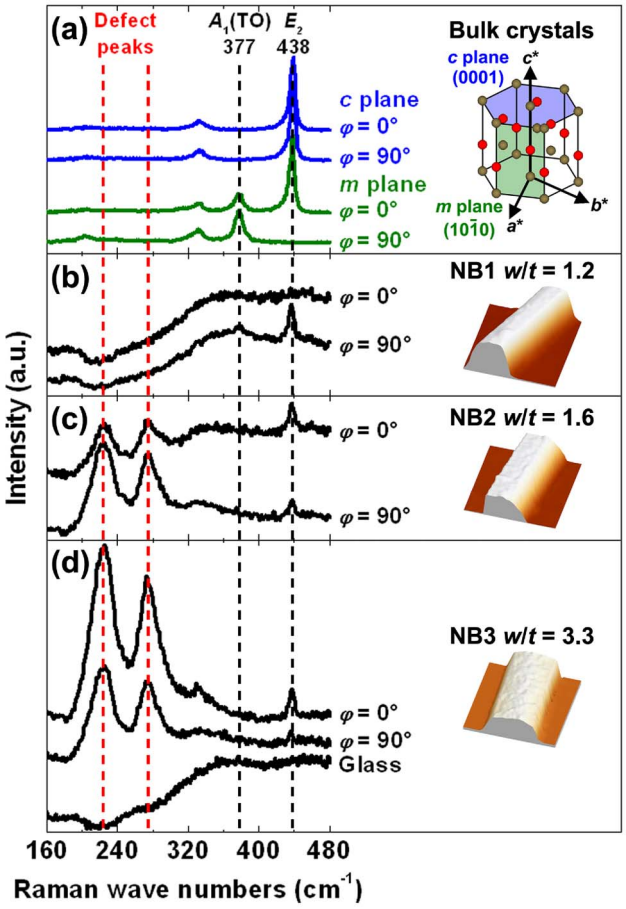

FIG. 2. (Color online) (a) PR spectra from the *c* and *m* planes of a ZnO crystal, shown in blue and green, respectively. The wurtzite structure (Zn atoms are brown, O atoms red) is also shown, where a^*, b^*, and c^* are the reciprocal lattice vectors. [(b)–(d)] AFM images (3×3 μm) of three NBs labeled NB1, NB2, and NB3 and corresponding PR spectra. In (d) a PR spectrum of the glass substrate is shown at the bottom. All the PR spectra in (a)–(d) are collected in the copolarized configuration for φ=0 and 90°. The spectra are offset vertically for clarity.

AQ: #3

polarization is rotated and the ZnO NB axis remained parallel or perpendicular to the analyzed scattered polarization (see supplementary information[25]). The exposure time for each Raman spectrum was 10 s for the bulk crystals and 20 min for NBs. After each rotation of the NBs, the laser spot is recentered on the same NB and at the same location along the NB.

Prior to the PR characterization of ZnO NBs, PR data were collected on the *c*-plane and *m*-plane of bulk ZnO crystals [Fig. 2(a)]. In ambient conditions, ZnO has a wurtzite structure (space group C_{6v}^4). Group theory predicts four Raman-active modes: one A_1, one E_1, and two E_2 modes.[11,20,23] The polar A_1 and E_1 modes split into transverse (TO) and longitudinal optical branches. On the *c*-plane (0001)-oriented sample, only the E_2 modes, at 99 (not shown) and 438 cm^{-1}, are observed, and their intensity is independent of the sample orientation φ [Fig. 2(a)]. On the *m*-plane (10$\bar{1}$0)-oriented sample, the E_2, E_1 (TO), and A_1 (TO) modes are observed at 99, 438, 409, and 377 cm^{-1}, respectively [Fig. 2(a)], and their intensity depends on φ. Peaks at 203 and 331 cm^{-1} in both crystals are assigned to multiple phonon scattering processes. The intensity, center, and width of the peaks at 438, 409, and 377 cm^{-1} were obtained by fitting the experimental PR spectra with Lorentzian lines (see supplementary information[25]). The successful fits of the angular dependencies by using the group theory and crystal symmetry[23] indicate that PR data can be used to characterize the growth direction of ZnO NBs. It is noted that the ZnO NBs studied here have dimensions over 300 nm, so the determination of the growth direction is not expected to be affected by any enhancement of the polarized Raman signal due to their high aspect ratio.[24]

AFM images and PR data of three individual ZnO NBs are presented in Figs. 2(b)–2(d). These NBs, labeled NB1, NB2, and NB3, have different dimensions and properties as summarized in Table I. A comparison of the PR spectra in Figs. 2(a)–2(d) reveals differences between bulk ZnO and individual NBs. First, the glass cover slip gives rise to a weak broadband centered around 350 cm^{-1} on the Raman spectra of the NBs [see bottom of Fig. 2(d)]. Second, there are additional Raman bands around 224 and 275 cm^{-1} for NB2 and NB3. These bands are observed in doped or ion-implanted ZnO crystals.[11,20] Their appearance is explained by the disorder in the crystal lattice due to randomly distributed point defects, such as oxygen vacancies or impurities. The defect peaks area increases in the order NB1 < NB2 < NB3. Since the laser spot diameter is larger than the width of all three NBs, but smaller than their length, *L*, the NB volume probed by the laser beam is approximated by the product of the width, *w*, with the thickness, *t*. The volume

TABLE I. Summary of the PR-AFM results for NB1, NB2, and NB3.

	w (nm)	*t* (nm)	*w*/*t*	*L* (μm)	θ (°)	*E* (GPa)	Defects
NB1	1080	875	1.2	40	28 ± 15	62 ± 5	No
NB2	1150	710	1.6	49	72 ± 15	38 ± 5	Yes
NB3	1510	455	3.3	59	66 ± 15	17 ± 5	Yes

probed decreases in the order NB1($w \times t = 9.45 \times 10^3$ nm^2) > NB2(8.17×10^3 nm^2) > NB3(6.87×10^3 nm^2). This indicates that the density of point defects is highest in NB3, and increases with the width to thickness ratio, w/t, in the order NB1 < NB2 < NB3.

The PR intensity variations of the 438 cm^{-1} peak as a function of φ in the various polarization configurations were fitted by using group theory and crystal symmetry to determine the angle θ between the NB long axis (or growth direction) and the c-axis ([0001] axis) of the constituting ZnO wurtzite structure[21,23] (see supplementary information[25]). Intensity variations of the 377 cm^{-1} peak, when present, are used to confirm the obtained values of θ. The results are shown in Table I and indicate that growth directions other than the most commonly observed c-axis are possible, particularly when point defects are present.

Finally, the elastic properties of NB1, NB2, and NB3 are characterized by AFM using the modulated nanoindentation method.[6,7,22] In a previous study, the elastic modulus of ZnO NBs was found to decrease with increasing w/t and this w/t dependence was attributed to the presence of planar defects in NBs with high w/t.[6,7] By using PR-AFM, we can study the role of randomly distributed defects, morphology, and growth direction on the elastic properties in the same individual ZnO NB. The measured elastic moduli, E, are 62 GPa for NB1, 38 GPa for NB2, and 17 GPa for NB3. These PR-AFM results confirm the w/t dependence of the elastic modulus in ZnO NBs, but more importantly they reveal that the elastic modulus of ZnO NBs can significantly decrease, down by almost one order of magnitude, with the presence of randomly distributed point defects.

In summary, a new approach combining polarized Raman spectroscopy and AFM reveals the strong influence of point defects on the elastic properties of ZnO NBs and their morphology. Based on a scanning probe, PR-AFM provides an *in situ* and nondestructive tool for the complete characterization of the crystal structure and the physical properties of individual nanostructures that can be in as-fabricated nanodevices.

The authors acknowledge the financial support from the Department of Energy under Grant No. DE-FG02-06ER46293.

[1] Y. Qin, X. Wang, and Z. L. Wang, Nature (London) **451**, 809 (2008).
[2] X. Wang, J. Song, J. Liu, and Z. L. Wang, Science **316**, 102 (2007).
[3] D. J. Müller and Y. F. Dufrêne, Nat. Nanotechnol. **3**, 261 (2008).
[4] H. Peng, C. Xie, D. T. Schoen, and Y. Cui, Nano Lett. **8**, 1511 (2008).
[5] U. Diebold, Surf. Sci. Rep. **48**, 53 (2003).
[6] M. Lucas, W. J. Mai, R. Yang, Z. L. Wang, and E. Riedo, Nano Lett. **7**, 1314 (2007).
[7] M. Lucas, W. J. Mai, R. Yang, Z. L. Wang, and E. Riedo, Philos. Mag. **87**, 2135 (2007).
[8] M. D. Uchic, D. M. Dimiduk, J. N. Florando, and W. D. Nix, Science **305**, 986 (2004).
[9] D.-S. Yang, C. Lao, and A. H. Zewail, Science **321**, 1660 (2008).
[10] M. Dienwiebel, G. S. Verhoeven, N. Pradeep, J. W. M. Frenken, J. A. Heimberg, and H. W. Zandbergen, Phys. Rev. Lett. **92**, 126101 (2004).
[11] Ü. Özgür, Ya. I. Alivov, C. Liu, A. Teke, M. A. Reshchikov, S. Doğan, V. Avrutin, S.-J. Cho, and H. Morkoç, J. Appl. Phys. **98**, 041301 (2005).
[12] Z. L. Wang, J. Phys.: Condens. Matter **16**, R829 (2004).
[13] G. R. Li, T. Hu, G. L. Pan, T. Y. Yan, X. P. Gao, and H. Y. Zhu, J. Phys. Chem. C **112**, 11859 (2008).
[14] Z. W. Pan, Z. R. Dai, and Z. L. Wang, Science **291**, 1947 (2001).
[15] P. Poncharal, Z. L. Wang, D. Ugarte, and W. A. De Heer, Science **283**, 1513 (1999).
[16] A. M. Minor, J. W. Morris, and E. A. Stach, Appl. Phys. Lett. **79**, 1625 (2001).
[17] B. Varghese, Y. Zhang, L. Dai, V. B. C. Tan, C. T. Lim, and C.-H. Sow, Nano Lett. **8**, 3226 (2008).
[18] M. Lucas and R. J. Young, Phys. Rev. B **69**, 085405 (2004).
[19] I. Calizo, A. A. Balandin, W. Bao, F. Miao, and C. N. Lau, Nano Lett. **7**, 2645 (2007).
[20] H. Zhong, J. Wang, X. Chen, Z. Li, W. Xu, and W. Lu, J. Appl. Phys. **99**, 103905 (2006).
[21] T. Livneh, J. Zhang, G. Cheng, and M. Moskovits, Phys. Rev. B **74**, 035320 (2006).
[22] I. Palaci, S. Fedrigo, H. Brune, C. Klinke, M. Chen, and E. Riedo, Phys. Rev. Lett. **94**, 175502 (2005).
[23] C. A. Arguello, D. L. Rousseau, and S. P. S. Porto, Phys. Rev. **181**, 1351 (1969).
[24] H. M. Fan, X. F. Fan, Z. H. Ni, Z. X. Shen, Y. P. Feng, and B. S. Zou, J. Phys. Chem. C **112**, 1865 (2008).
[25] See EPAPS supplementary material at http://dx.doi.org/10.1063/1.3177065 for ■.

AQ: #1
AQ: #2

AUTHOR QUERIES — 074928APL

#1 Au: Please check accuracy of year in Ref. 17
#2 Au: Please supply brief description of supplementary material in Ref. 25
#3 Au: Although a caption makes reference to color online, figures will appear black and white in print. Please make sure the caption makes sense to print reader